



# Dithienobenzochalcogenodiazole-based electron donor–acceptor polymers for organic electronics



Amsalu Efrem<sup>a</sup>, Yanlian Lei<sup>b</sup>, Bo Wu<sup>b</sup>, Mingfeng Wang<sup>a,\*</sup>, Siu Choon Ng<sup>d,\*\*</sup>, Beng S. Ong<sup>c,\*\*\*</sup>

<sup>a</sup> School of Chemical and Biomedical Engineering, Nanyang Technological University, 62 Nanyang Drive, 637459, Singapore

<sup>b</sup> Department of Physics, Research Centre of Excellence for Organic Electronics and Institute of Advanced Materials, Hong Kong Baptist University, Kowloon Tong, Kowloon, Hong Kong

<sup>c</sup> Research Centre of Excellence for Organic Electronics, Institute of Creativity and Department of Chemistry, Hong Kong Baptist University, Kowloon Tong, Kowloon, Hong Kong

<sup>d</sup> Singapore Institute of Technology, 10 Dover Drive, 138683, Singapore

## ARTICLE INFO

### Article history:

Received 13 December 2015

Received in revised form

29 January 2016

Accepted 31 January 2016

Available online 18 February 2016

### Keywords:

Dithienobenzochalcogenodiazole

Electron donor-acceptor polymers

Field-effect transistors

Field-effect mobility

Organic photovoltaics

## ABSTRACT

Apositely functionalized dithienobenzo-thiadiazole and dithienobenzo-oxadiazole-monomers were prepared and used in the synthesis of conjugated electron donor-acceptor (D-A) polymers. Detailed systematic investigations were carried out to study the effects of chalcogen atoms and three donor units on the optical and electrochemical properties as well as photovoltaic and field-effect transistor performance of the D-A polymers. All polymers displayed good thermal properties. Polymers containing benzooxadiazole moiety showed deeper LUMO levels as compared to their benzothiadiazole-containing analogues, whereas those derived from weak donor unit exhibited deeper HOMO levels than those with stronger donors. Photovoltaic power conversion efficiency of over 2% and hole field-effect mobility of  $2.6 \times 10^{-2} \text{ cm}^2 \text{ V}^{-1} \text{ s}^{-1}$  and on/off ratio of over  $10^5$  were obtained. These results demonstrate that dithienobenzo-chalcogenodiazole structures are potentially useful electron acceptor building blocks for the construction of D-A polymers for organic electronics applications.

© 2016 Elsevier Ltd. All rights reserved.

## 1. Introduction

Research on organic semiconductors has advanced rapidly over the past decade owing to their potential as electrically active materials in producing low-cost, light weight, large area, and flexible electronic devices such as organic light-emitting diodes (OLEDs), organic photovoltaic (OPVs), and organic field-effect transistors (OFETs) [1–3]. Structurally, organic semiconductors can be readily modified to tune molecular properties such as crystallinity, energy levels, optical band gap, etc. to achieve desirable electrical performance characteristics [4–7]. Thus, understanding the relationships between molecular structure, material properties, and device performance would enable rational materials design for improved

device performance. From these perspectives, conjugated electron donor and acceptor (D-A) polymers have been a plausible structural design strategy to achieve the required materials properties through controlled intramolecular charge transfer from the donor to acceptor moiety within the polymer framework [8].

Chalcogenodiazole chromophore has received great interest as an electron acceptor moiety for the construction of D-A polymers for organic electronics applications. Many known D-A polymers utilize 2,1,3-benzothiadiazole (BTz) structure [9–12], which has high electron affinity and relatively low HOMO level as compared to other acceptor moieties [13–16]. D-A polymers with the BTz moiety modified via substitution of sulfur with other heteroatoms have led to interesting D-A systems, offering enhanced OPVs and OFET performance characteristics [17–21]. Using BTz-based D-A polymers as donors, Liu et al. has recently reported PCE as high as over 10% in OPV devices [22].

Another design modification of the BTz moiety in D-A polymers is through fusion of its benzo function with other aromatics to maximize  $\pi$ -orbital overlap by restricting intramolecular rotation such as to induce optimal face-to-face  $\pi$ - $\pi$  stacking and thus to

\* Corresponding author.

\*\* Corresponding author.

\*\*\* Corresponding author.

E-mail addresses: [mfwang@ntu.edu.sg](mailto:mfwang@ntu.edu.sg) (M. Wang), [SiuChoon.Ng@SingaporeTech.edu.sg](mailto:SiuChoon.Ng@SingaporeTech.edu.sg) (S.C. Ng), [bong@hkbu.edu.hk](mailto:bong@hkbu.edu.hk) (B.S. Ong).

facilitate charge transport *via* intermolecular hopping [23–26]. Thus, some of recent works on fusion of BTz moiety with thiophene, indole, and thieno[3,2-b]pyrrole have shown significant improvements in physical, electrochemical and device properties of the resulting polymers [27–34]. D-A polymers derived from another acceptor structure, benzooxadiazole (BOz) have also been shown to exhibit enhanced electronic device performance [35–42]. To the best of our knowledge, few D-A small molecules and polymers based on thiophene-fused-benzooxadiazole have been reported for organic electronics applications [43,44].

In this work, we report the synthesis and optoelectronic characterization of five D-A copolymers based on two acceptor units, dithieno[3',2':3,4; 2'',3'':5,6]benzo[1,2-c] [1,2,5] thiodiazole (DT-BTD) and dithieno[3',2':3,4; 2'',3'':5,6] benzo [1,2-c] [1,2,5] oxadiazole (DT-BOD), alternating with three donor moieties, thienothiophene (TT), bithiophene (BT), and alkylidene-fluorene [45]. We also studied the effects of chalcogen atoms (S and O) on their physicochemical properties and OPV and OFET device performances.

## 2. Experimental section

### 2.1. Materials

Unless stated otherwise, all starting materials were obtained from Sigma–Aldrich and used without further purification. The anhydrous solvents like tetrahydrofuran (THF), diethyl ether, and toluene for the reaction were collected from PureSolv MD solvent purification system of model PS-400-5-MD. Compound 5, 6, 7a, and 7b were prepared according reported procedures [46]. All the reactions were carried out under nitrogen atmosphere.

### 2.2. Characterization

<sup>1</sup>H NMR spectra were recorded on a Bruker AV 300 spectrometer with TMS as the internal reference. Chemical shifts of <sup>1</sup>H NMR were reported in ppm. Splitting patterns were designated as s (singlet), d (doublet), t (triplet), m (multiplet), and br (broad). Molecular weights of the polymers were obtained on a Gel permeation chromatography (GPC) using CHCl<sub>3</sub> at 80 °C as eluent after calibration with standard polystyrene. Elemental analyses were performed on a Vario EL elemental analysis instrument (Elementar). UV–vis absorption spectra were recorded on a Cary 4000 spectrophotometer. Thermogravimetric analysis (TGA) was carried out on a Perkin Elmer Diamond TGA/DTA, at a heating rate of 10 °C min<sup>-1</sup> from 25 to 600 °C under a nitrogen atmosphere. Cyclic voltammetry (CV) measurements were conducted on a three-electrode electrochemistry workstation (Model CHI006D) in 0.1 M anhydrous acetonitrile solution of tetrabutylammonium hexafluorophosphate (Bu<sub>4</sub>NPF<sub>6</sub>) at 25 °C under nitrogen atmosphere. A glassy carbon disk coated with a thin layer of polymer film was used as working electrode, a silver wire as pseudo-reference electrode and a platinum wire as counter electrode. Tapping-mode AFM height images (5 × 5 μm<sup>2</sup>) of pristine polymer films on OTS-modified Si/SiO<sub>2</sub> substrates for all polymers annealed at 120 °C were taken by using scanning probe microscope (SPM) digital instrument dimension V.

### 2.3. OPV fabrication and characterization

The photovoltaic properties of all polymers were investigated using bulk heterojunction organic photovoltaics (BHJ-OPVs) with configuration of ITO/ZnO/active layer/MoO<sub>3</sub>/Ag, where the active layer was composed of D-A polymers as electron donor and PCBM as an electron acceptor. For all polymers, ZnO was fabricated by spin coating, while MoO<sub>3</sub> and Ag were fabricated by thermal evaporation.

The measurements of photovoltaic performances were carried out under illumination of AM1.5G simulated solar light at 940 W m<sup>-2</sup>. Thus the PCE is calculated as Voc\*Jsc\*FF/0.94. All of the polymers with concentration of 10 mg/mL were mixed with PC<sub>70</sub>BM in wt. ratio of 1:2, and dissolved in the chlorobenzene (CB) solvent with 3% of 1,8-diiodooctane (DIO) as an additive for spin-coating at 500 and 1000 rpm, where the photovoltaic properties of active layer prepared at 500 rpm is described in the supporting information.

### 2.4. OFET fabrication and characterization

OFET performance characteristics of all polymers were studied using a bottom gate, top contact configuration fabricated on heavily n-doped silicon wafer <100> with a 300-nm thermally grown SiO<sub>2</sub> as substrate/gate electrode. The SiO<sub>2</sub>/Si wafer substrate was first modified with OTS-8 (or OTS-18) [8]. Then, a solution of D-A polymer dissolved in chlorobenzene (3 mg/mL) was spin coated on SiO<sub>2</sub> gate dielectric at a spin speed of 800 rpm for 120 s in glove box. Subsequently, the resulting polymer film was placed into a vacuum oven to remove the solvent. A series of gold source/drain electrode pairs were deposited on top of the polymer film by vacuum thermal evaporation through a shadow mask to create a set of OFET devices. All of the devices were evaluated in ambient condition using a dual-channel Keithley 2636B SourceMeter. The FET mobility was extracted using the following equation in the saturation regime from the gate sweep:  $I_{ds} = \mu C_i (V_g - V_{th})^2 (W/2L)$ .

Where  $I_{ds}$  is the drain current,  $\mu$  is the field-effect mobility,  $C_i$  (10 nF cm<sup>-2</sup>) is the capacitance per unit area of the gate dielectric layer, and  $V_g$  and  $V_{th}$  are gate voltage and threshold voltage.  $V_{th}$  was derived from the relationship between the square root of  $I_{ds}$  at the saturated regime and  $V_g$  by extrapolating the measured data to  $I_{ds} = 0$ .  $W$  (1500 μm) and  $L$  (160 or 80 μm) are channel width and length, respectively.

### 2.5. Synthesis of monomers

#### 2.5.1. Synthesis of 5,8-dibromodithieno [3',2':3,4; 2'',3'':5,6]benzo [1,2-c] [1,2,5] thiodiazole (**8a**)

To a 250-mL round-bottom flask, equipped with a stir bar and a condenser was added DT-BTD (0.623 g, 2.5 mmol, 1 equiv), chloroform (200 mL), and bromine (0.282 mL, 0.8819 g, 5.519 mmol, 2.2 equiv.). The reaction mixture was warmed to 80–85 °C, and stirred for 12 h. The reaction mixture was cooled to room temperature, and the resulting solid was filtered. The filtrate cake was collected, dried, and recrystallized from *o*-dichlorobenzene, to give **8a** as yellow crystalline solid (0.76 g, 75% yield). <sup>1</sup>H NMR (300 MHz, hot-chlorobenzene-*d*):  $\delta$  (ppm): 7.95 (s, 2H).

#### 2.5.2. Synthesis of 5,8-dibromodithieno[3',2':3,4; 2'',3'':5,6]benzo [1,2-c]oxadiazole (**8b**)

The reaction was carried using the same procedure as **8a**. The workup has been modified as follows: after 12 h of reaction it was allowed to cool to room temperature, while cooling the mixture was diluted with aqueous Na<sub>2</sub>S<sub>2</sub>O<sub>3</sub> solution. Subsequently, the mixture was separated and washed with saturated aqueous NaHCO<sub>3</sub> solution and brine. Then dried over MgSO<sub>4</sub>, filtered and concentrated under vacuum, and the solid product was recrystallized from *o*-dichlorobenzene to give **8b** as a yellow crystalline solid (69% yield). <sup>1</sup>H NMR (300 MHz, CDCl<sub>3</sub>)  $\delta$  (ppm): 7.92 (s, 2H).

#### 2.5.3. Synthesis of 5,8-bis(4-(2-octyldodecyl) thiophen-2-yl) dithieno [3',2':3,4; 2'',3'':5,6] benzo[1,2-c] [1,2,5]thiodiazole (**9a**)

Compound 8 (0.2 g, 0.492 mmol) and Compound 4 (0.675 g, 1.28 mmol) were added to 40 mL toluene in a 100 mL round-bottom flask and purged with N<sub>2</sub> for 30 min. Pd(PPh<sub>3</sub>)<sub>4</sub> (29 mg,

0.025 mmol) was added to the mixture and refluxed for 48 h. After the mixture was cooled to room temperature, the solvent was evaporated under reduced pressure, and then dissolved in 50 mL diethyl ether and extensively washed with water and brine. The organic phase was separated and dried over anhydrous  $\text{MgSO}_4$ . After removal of the solvent by vacuum evaporation, the residue was purified by column chromatography on silica gel ( $\text{CH}_2\text{Cl}_2/\text{hexane} = 1:10$ ) to give Compound **9** as a yellow oil (0.34 g, 71%).

$^1\text{H NMR}$  (300 MHz,  $\text{CDCl}_3$ )  $\delta$  (ppm): 8.0 (d, 2H), 7.15 (s, 2H), 6.90 (s, 2H), 2.57 (d, 4H), 1.65 (br, 2H), 1.38–1.13 (m, 64H), 0.92–0.81 (m, 12H).

#### 2.5.4. Synthesis of 5,8-bis(4-(2-octyldodecyl) thiophen-2-yl) dithieno[3',2':3,4; 2'',3'':5,6] benzo[1,2-c] [1,2,5] oxadiazole (**9b**)

Compound **9b** was synthesized in the same procedure with Compound **9a**. Yield: 84%.

$^1\text{H NMR}$  (300 MHz,  $\text{CDCl}_3$ )  $\delta$  (ppm): 7.90 (d, 2H), 7.15 (d, 2H), 6.92 (d, 2H), 2.55 (d, 4H), 1.64 (br, 2H), 1.38–1.13 (m, 64H), 0.92–0.8 (m, 12H).

#### 2.5.5. Synthesis of 5,8-bis(5-bromo-4-(2-octyl dodecyl)thiophen-2-yl)dithieno [3',2': 3,4; 2'',3'': 5,6]- benzo [1,2-c] [1,2,5]thiadiazole (**10a**)

N-Bromosuccinimide (0.137 g, 0.768 mmol) was added portion-wise to a solution of Compound **9** (0.34 g, 0.349 mmol) in 80 mL of THF at room temperature. After the mixture was stirred for 12 h,  $\text{NaHCO}_3$  solution was added, and the mixture was extracted with  $\text{CH}_2\text{Cl}_2$ . The organic layer was washed with water and brine and then dried over anhydrous  $\text{MgSO}_4$ . The solvent was removed by vacuum evaporation, and the residue was purified by column chromatography on silica gel ( $\text{CH}_2\text{Cl}_2/\text{hexane} = 1:10$ ) to give Compound **10a** as a yellow oil (0.277 g, 70%).

$^1\text{H NMR}$  (300 MHz,  $\text{CDCl}_3$ )  $\delta$  (ppm): 7.92 (s, 2H), 6.99 (s, 2H), 2.52 (d, 4H), 1.70 (br, 2H), 1.38–1.12 (m, 64H), 0.93–0.78 (m, 12H).

#### 2.5.6. Synthesis of 5,8-bis(5-bromo-4-(2-octyl dodecyl)thiophen-2-yl)dithieno [3',2': 3,4; 2'',3'': 5,6]- benzo [1,2-c] [1,2,5]oxadiazole (**10b**)

Compound **10b** was synthesized in the same procedure with Compound **10a**. Yield: 92%.

$^1\text{H NMR}$  (300 MHz,  $\text{CDCl}_3$ )  $\delta$  (ppm): 7.80 (s, 2H), 6.97 (s, 2H), 2.52 (d, 4H), 1.69 (br, 2H), 1.41–1.02 (m, 64H), 0.94–0.76 (m, 12H).

### 2.6. Synthesis of D-A polymers by Stille polycondensation

To a 25 mL round-bottom flask dibromide monomer (0.1 mmol), bis(trimethylstannyl)-substituted monomers (0.1 mmol), and dry toluene (4 ml) were added. After degassed by  $\text{N}_2$  for 15 min,  $\text{Pd}(\text{PPh}_3)_4$  (3 mol%) was added under nitrogen stream and degassed via nitrogen bubbling for about 30 min. Then, the reaction mixture was heated to 110 °C and stirred for 3 days. After being cooled to room temperature, the reaction mixture was poured into 100 mL of methanol and filtered. The resulted crude product was then subjected to Soxhlet extraction with methanol, acetone, hexane, and chloroform in sequence. The chloroform fraction was evaporated to dryness and reprecipitated from methanol to give **P1**, **P2** and **P3** as a black powder.

#### 2.6.1. Poly[5-(4-(2-methyldodecyl)-5-(thieno[3,2-b]thiophen-2-yl)thiophen-2-yl)-8-(4-(2-octyldodecyl)thiophen-2-yl)dithieno [3',2':3,4;2'',3'':5,6]benzo[1,2-c] [1,2,5]thiadiazole] (**P1**)

Yield: 68%. Anal. Calcd for  $\text{C}_{64}\text{H}_{90}\text{N}_2\text{S}_7$ : C, 69.13; H, 8.16; N, 2.52; S, 20.19. Found: C, 65.36; H, 7.529; N, 3.077; S, 22.05.

#### 2.6.2. Poly[5-(3-(2-methyldodecyl)-[2,2':5',2''-terthiophen]-5-yl)-8-(4-(2-octyldodecyl)thiophen-2-yl)-dithieno[3',2':3,4;2'',3'': 5,6] benzo[1,2-c] [1,2,5]thiadiazole] (**P2**)

Yield: 47%. Anal. Calcd for  $\text{C}_{66}\text{H}_{92}\text{N}_2\text{S}_7$ : C, 69.66; H, 8.15; N, 2.46; S, 19.73. Found: C, 67.55; H, 8.375; N, 2.421; S, 19.77.

#### 2.6.3. Poly[5-(4-(2-methyldodecyl)-5-(thieno[3,2-b]thiophen-2-yl)thiophen-2-yl)-8-(4-(2-octyldodecyl)thiophen-2-yl)dithieno [3',2':3,4;2'',3'':5,6]benzo[1,2-c] [1,2,5]oxadiazole] (**P3**)

Yield: 41%. Anal. Calcd for  $\text{C}_{64}\text{H}_{90}\text{N}_2\text{OS}_6$ : C, 70.15; H, 8.28; N, 2.56; O, 1.46; S, 17.56. Found: C, 65.96; H, 7.854; N, 2.813; S, 18.33.

### 2.7. Synthesis of D-A polymers by Suzuki polycondensation

To a 25- mL round-bottom flask dibromide monomer (0.1 mmol), 2,2'-(9-(heptadecan-9-ylidene)-9H-fluorene-2,7-diyl) bis (4,4,5,5-tetramethyl-1,3,2-dioxaborolane (0.1 mmol), and dry toluene (4 mL), and 2 M  $\text{K}_2\text{CO}_3$  aqueous solution (1 mL) were added. After degassed by  $\text{N}_2$  for 15 min,  $\text{Pd}(\text{PPh}_3)_4$  (~3 mol%) was added under nitrogen stream and degassed via nitrogen bubbling for about 30 min. Then, the reaction mixture was heated to 110 °C and stirred for 3 days. After being cooled to room temperature, the reaction mixture was poured into 100 mL of methanol and filtered. The resulting crude product was then subjected to Soxhlet extraction with methanol, acetone, hexane, and chloroform in sequence. The chloroform fraction was evaporated to dryness and reprecipitated from methanol to give **PF-O** as a dark red and **PF-S** were collected from hexane fraction and reprecipitated in methanol to give an orange-red solid.

#### 2.7.1. Poly[5-(5-(9-(heptadecan-9-ylidene)-9H-fluorene-2-yl)-4-(2-octyldodecyl)thiophen-2-yl)-8-(4-(2-octyldodecyl)thiophen-2-yl) dithieno[3',2':3,4;2'',3'':5,6]benzo[1,2-c] [1,2,5]thiadiazole] (**PF-S**)

Yield: 69%. Anal. Calcd for  $\text{C}_{88}\text{H}_{128}\text{N}_2\text{S}_5$ : C, 76.91; H, 9.39; N, 2.04; S, 11.67. Found: C, 68.37; H, 9.246; N, 1.871; S, 9.666.

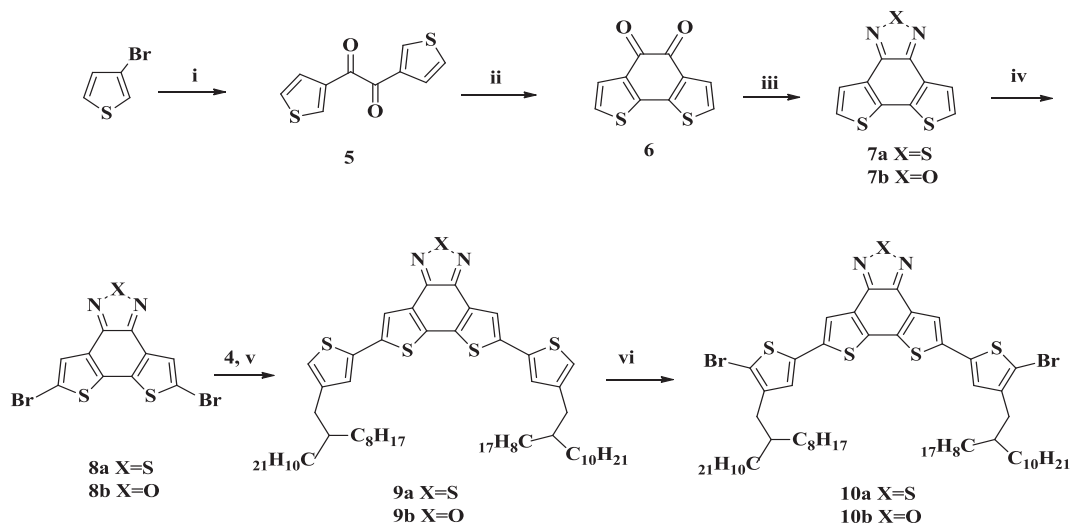
#### 2.7.2. Poly[5-(5-(9-(heptadecan-9-ylidene)-9H-fluorene-2-yl)-4-(2-octyldodecyl)thiophen-2-yl)-8-(4-(2-octyldodecyl)thiophen-2-yl) dithieno[3',2':3,4;2'',3'':5,6]benzo[1,2-c] [1,2,5]oxadiazole] (**PF-O**)

Yield: 82%. Anal. Calcd for  $\text{C}_{88}\text{H}_{128}\text{N}_2\text{OS}_4$ : C, 77.82; H, 9.50; N, 2.06; O, 1.18; S, 9.44. Found: C, 76.48; H, 10.05; N, 2.172; S, 9.302.

## 3. Results and discussion

### 3.1. Synthesis of monomers and D-A polymers

The syntheses of monomers, **10a** and **10b**, are depicted in [Scheme 1](#). The intermediate **7a** was synthesized in 79% yield from the diketone **6** [46] via derivatization to its corresponding diamine followed by  $\text{SOCl}_2$  treatment. The intermediate **7b** was obtained from the same diketone **6** by refluxing it with hydroxyl amine-hydrochloride in a pressure vessel at 140 °C for 3 days to get a yellow solid. Bromination of **7a** and **7b** with  $\text{Br}_2$  provided the corresponding dibromides, **8a** (75% yield) and **8b** (69% yield), respectively. While **8a** and **8b** had limited solubility in common organic solvents except dichlorobenzene, hot chlorobenzene, and toluene, their respective bis[4-(2-octyldodecyl)-2-thienyl]-functionalized products, **9a** and **9b** exhibited greatly improved solubility characteristics. Subsequent bromination provided the respective dibromides, **10a** and **10b**. The chemical identities of all the intermediates **1** to **10** in [Scheme 1](#) were confirmed using NMR spectroscopy. The synthesis of 4-(2-octyldodecyl)-2-(trimethylstannyl)thiophene for the conversion of **8** to **9** is depicted in [Scheme S1 \(Supporting information\)](#). Its synthesis could not be accomplished via the usual Kumada cross-coupling reaction, mostly likely due to steric



**Scheme 1.** Synthesis of acceptor monomers (i) *n*-BuLi,  $-78\text{ }^{\circ}\text{C}$ , CuBr/LiBr then oxalyl chloride, THF, 78%. (ii) FeCl<sub>3</sub>, CH<sub>2</sub>Cl<sub>2</sub>, r.t., 82%. (iii) **7a**) HONH<sub>2</sub>·HCl, 10% Pd/C,  $78\text{ }^{\circ}\text{C}$  then N<sub>2</sub>H<sub>4</sub>·H<sub>2</sub>O,  $-60\text{ }^{\circ}\text{C}$ , EtOH, 34%, then SOCl<sub>2</sub>, Et<sub>3</sub>N, DCM, reflux, 79%. (iii) **7b**) HONH<sub>2</sub>·HCl,  $85\text{ }^{\circ}\text{C}$  for 24 h then,  $140\text{ }^{\circ}\text{C}$  for 60hr, EtOH, 30%. (iv) Br<sub>2</sub>, CHCl<sub>3</sub>, reflux, 75% for **8a** and 69% for **8b**. (v) Pd(PPh<sub>3</sub>)<sub>4</sub>, toluene,  $110\text{ }^{\circ}\text{C}$ . 71% for **9a** and 84% for **9b** (vi) NBS, THF, r.t. 70% for **10a** and 92% for **10b**.

interference from the long branched alkyl chain. Instead, it was obtained from the Grignard reaction (*i*-prMgCl·LiCl complex) of 3-bromothiophene with 2-octyldodecyl aldehyde, followed by dehydroxylation with AlH<sub>3</sub> generated in situ from a mixture of LiAlH<sub>4</sub>–AlCl<sub>3</sub> and stannylation with Sn(Me)<sub>3</sub>Cl.

The D-A polymers, **P1**, **P2**, and **P3** were synthesized via Stille polycondensation of intermediate **10** and 2,5-bis(trimethyl stannyl)-thieno[3,2-*b*]thiophene or 5,5'-bis(trimethyl-stannyl)-2,2'-bithiophene, while both **PF-S** and **PF-O** were obtained from Suzuki polycondensation between intermediate **10** and dioxaborolan-alkylidene-fluorene in the presence of Pd(PPh<sub>3</sub>)<sub>4</sub> catalyst in refluxing toluene ( $110\text{ }^{\circ}\text{C}$ ) for 72 h. All D-A polymer products were isolated *via* precipitation from methanol and purified by sequential Soxhlet extractions with methanol, acetone, hexane, and chloroform. All of the D-A polymers have displayed relatively good solubility in chlorinated solvents such as chloroform and chlorinated benzene.

D-A polymers, **P1** and **P2**, which were utilized in our OFET studies, were obtained by our previous synthesis procedure as depicted in Scheme 2 [34]. First, 2-bromo-3-(2-octyldodecyl) thiophene were coupled with the donor units 2,5-bis(trimethyl stannyl)-thieno[3,2-*b*]thiophene or 5,5'-bis(trimethylstannyl)-2,2'-bithiophene followed by stannylation and Stille polycondensation with **8a**, though the molecular weights and overall reaction yields of the polymers were lower as compared to the one obtained by using Scheme 3.

The molecular weights and polydispersity index (PDI) of the D-A polymers were determined by gel permeation chromatography (GPC) at  $80\text{ }^{\circ}\text{C}$  with a polystyrene standard calibration and CHCl<sub>3</sub> as the eluent. As shown in Table 1, most D-A polymers have the weight-average molecular weights ( $M_w$ ) as high as 20 kDa and number-average molecular weight ( $M_n$ ) ranging from 5.4 to 12.6 kDa. The polydispersity index (PDI) for all the polymers is relatively narrow, except **P1** which shows a relatively broad PDI of 2.54 which might be due to its strong tendency to aggregate in solution as evidenced by its solution UV–vis absorption spectra (Fig. S2 of Supporting Information).

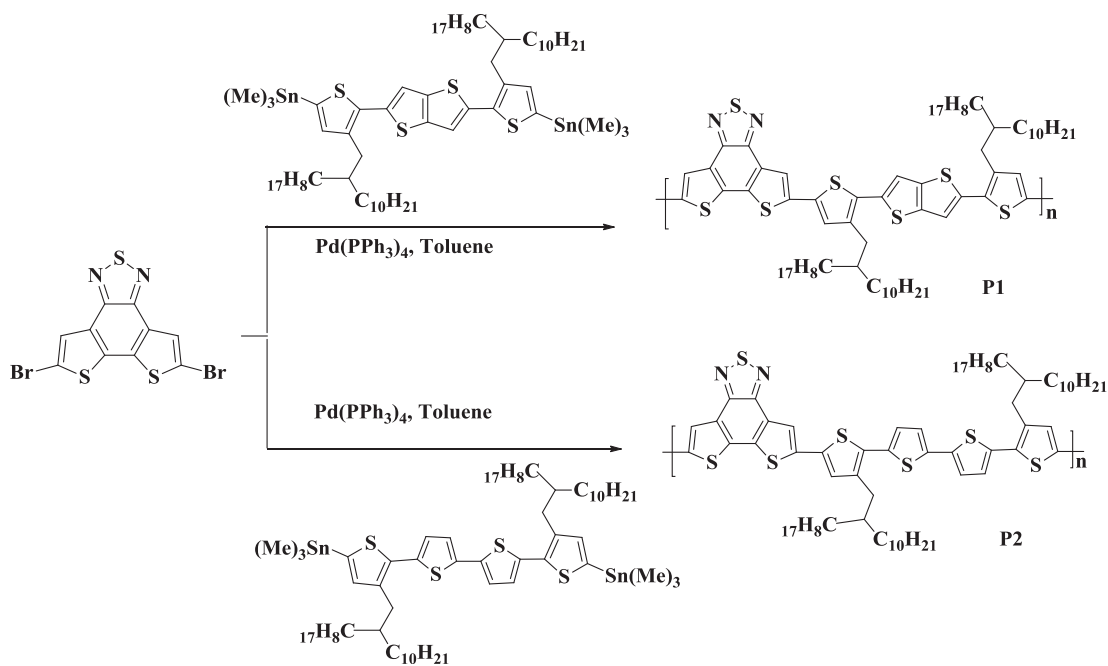
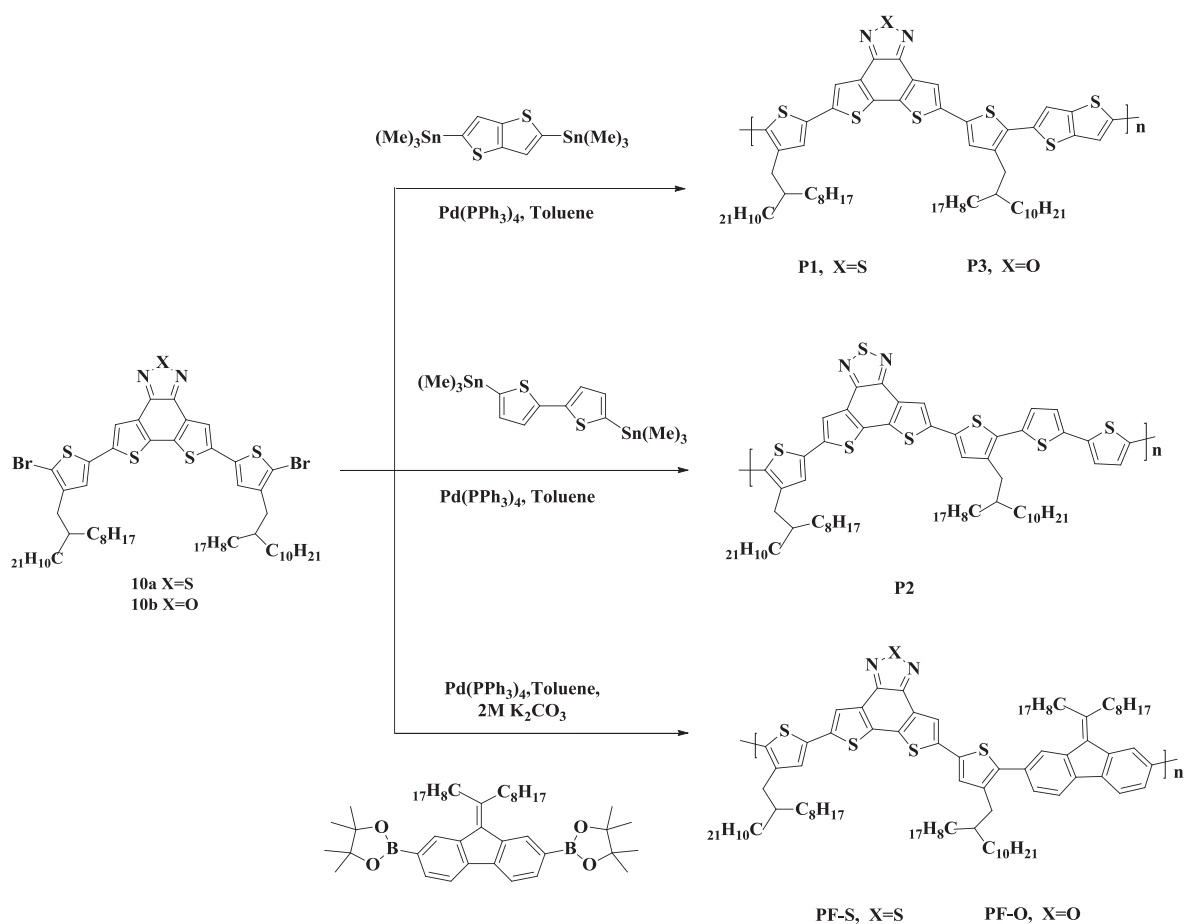
### 3.2. Thermal properties

Thermal stability of all D-A polymers was investigated by thermogravimetric analysis (TGA) at a heating rate of  $10\text{ }^{\circ}\text{C min}^{-1}$  under

nitrogen. Fig. 1 shows TGA where the onset decomposition temperature ( $T_d$ ) with 5% weight loss is in a range of  $316\text{--}416\text{ }^{\circ}\text{C}$ , indicating that all polymers have excellent thermal stability for use in optoelectronic devices such as OPVs and OFETs.

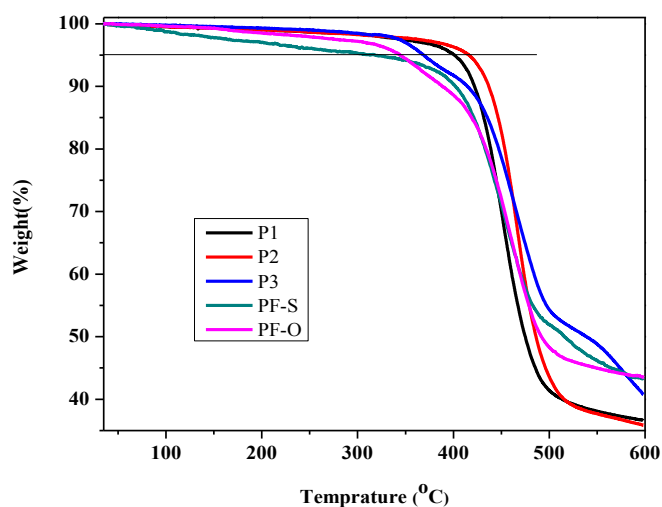
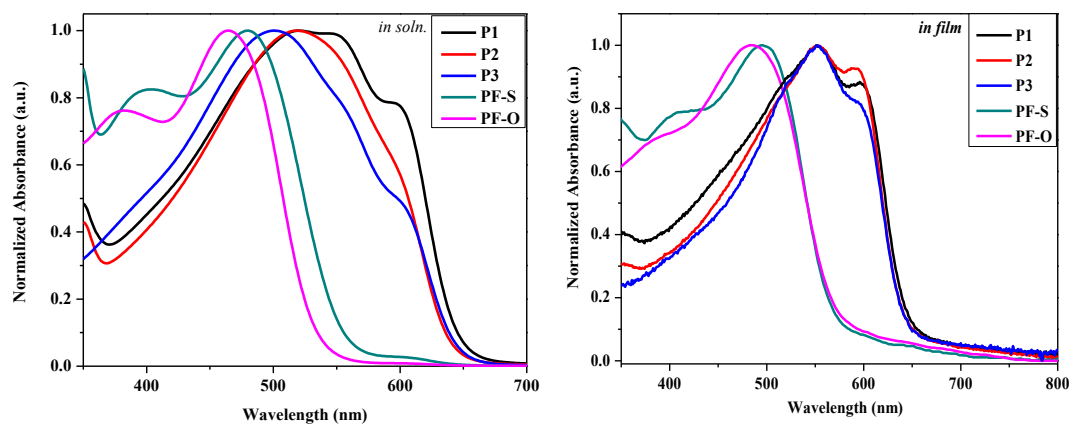
### 3.3. Optical properties

The absorption spectra of the D-A polymers in dilute chloroform solutions and spin-coated films on quartz substrates are shown in Fig. 2, while their respective optical data, including the maximum absorption peak wavelengths ( $\lambda_{\text{max}}$ ), absorption edge wavelengths ( $\lambda_{\text{onset}}$ ), shoulder maximum absorption peak wavelengths ( $\lambda_{\text{shoulder}}$ ), and optical band gap ( $E_g^{\text{opt}}$ ; calculated from  $\lambda_{\text{onset}}$ ), are summarized in Table 2. The significant red-shift and broad absorption bands of **P1–3** compared to those of **PF-S** and **PF-O** could be attributed to the strong intramolecular charge transfer (ICT) interaction between the electron-rich moieties and electron-deficient segments in the former polymers. The absorption maxima for **P1**, **P2**, and **P3** are 522, 520, 500 nm respectively and all of them displayed two shoulder peaks at ca. 560 and 600 nm, suggesting polymer aggregation even in solution (Fig. S2 of supporting information) [30]. The solution absorption maxima of **PF-S** and **PF-O** were at shorter wavelength region owing to the weaker electron acceptor strength of alkylidene-fluorene moiety. In thin films, as expected, all polymers (**P1**, **P2**, **P3**, **PF-S**, and **PF-O**) showed redshifts for up to ca. 15–53 nm, indicating higher molecular orders from intermolecular  $\pi$ - $\pi$  stacking interactions. Specifically, the oxadiazole-based polymers (**P3** and **PF-O**) exhibited larger redshifts than their corresponding thiadiazole-based counterparts (**P1** and **PF-S**), likely due to decreased steric interference to molecular interaction from the oxygen-containing oxadiazole-based moiety as compared to larger sulfur-containing thiadiazole-based moiety [47]. Furthermore, increased intensity of 0-0 vibrational peaks ( $\sim 600\text{ nm}$ ) relative to those of the 0-1 vibrational peaks was observed in the film spectra of **P1**, **P2**, and **P3**, suggesting relatively planar polymer backbone structures and formation of J-aggregates [47,48]. Finally, the absorption edges ( $\lambda_{\text{onset}}$ ) of film spectra of **P1**, **P2**, and **P3** were in the range of 650–660 nm, which correspond to an optical band gap ( $E_g^{\text{opt}}$ ) of 1.89 eV while  $\lambda_{\text{onset}}$  for **PF-S** and **PF-O** is about 580 nm, corresponding to  $E_g^{\text{opt}}$  of 2.1 eV.

Scheme 2. Previous synthetic route to D-A polymers, **P1** and **P2**.Scheme 3. Improved synthetic route to D-A polymers, **P1**, **P2**, **P3**, **PF-S** and **PF-O**.

**Table 1**  
Molecular weights and thermal properties of D-A polymers.

D-A Polymer	Yield (%)	<sup>a</sup> M <sub>n</sub> (× 10 <sup>3</sup> g/mol)	<sup>a</sup> M <sub>w</sub> (× 10 <sup>3</sup> g/mol)	<sup>a</sup> PDI	<sup>b</sup> T <sub>d</sub> (°C)
P1	68	8.0	20.5	2.54	401
P2	47	9.1	17.3	1.89	416
P3	41	7.6	14.8	1.93	368
PF-S	70	12.6	17.9	1.42	316
PF-O	82	5.4	8.6	1.59	343

<sup>a</sup> Determined by GPC in CHCl<sub>3</sub> at 80 °C using polystyrene standards.<sup>b</sup> Decomposition temperature, determined by TGA in nitrogen, based on 5% weight loss.**Fig. 1.** TGA plots of the five D-A polymers with a heating rate of 10 °C min<sup>-1</sup> under nitrogen.**Fig. 2.** UV-vis absorption spectra of D-A polymers in chloroform solution and thin films for D-A polymers, P1, P2, P3, PF-S, and PF-O.**Table 2**  
Optical data of the D-A polymers.

D-A Polymer	Solution			Film			
	<sup>a</sup> λ <sub>max</sub> [nm]	<sup>b</sup> λ <sub>should</sub> [nm]	<sup>c</sup> λ <sub>onset</sub> [nm]	<sup>a</sup> λ <sub>max</sub> [nm]	<sup>b</sup> λ <sub>should</sub> [nm]	<sup>c</sup> λ <sub>onset</sub> [nm]	<sup>d</sup> E <sub>g</sub> <sup>opt</sup> (eV)
P1	522	597	660	552	597	658	1.88
P2	520	600	651	552	592	654	1.89
P3	500	601	655	553	595	655	1.89
PF-S	480	—	570	495	—	578	2.15
PF-O	465	—	547	485	—	581	2.13

<sup>a</sup> Absorption maxima.<sup>b</sup> Absorption maxima at shoulder peak.<sup>c</sup> The onset edge absorption.<sup>d</sup> Estimated from the onset edge of absorption in films (λ<sub>onset</sub>): E<sub>g</sub><sup>opt</sup>(eV) = 1240/λ<sub>onset</sub> [nm].

### 3.4. Electrochemical properties

The cyclic voltammetry (CV) experiment were carried out on D-A polymer films to examine their electronic energy levels (Fig. S1, Supporting Information). The highest occupied molecular orbital (HOMO) and lowest unoccupied molecular orbital (LUMO) energy levels were calculated from the onset oxidation potentials (E<sub>ox</sub><sup>onset</sup>) and the onset reduction potentials (E<sub>red</sub><sup>onset</sup>) [49], respectively and summarized in Table 3. Within experimental errors, the band gaps calculated from the measured CV (E<sub>g</sub><sup>elc</sup>) data were essentially similar to those estimated from optical absorption edges (Table 2). It is obvious that the replacement of sulfur atom of thiadiazole moiety with oxygen atom to form oxadiazole moiety had a noticeable effect on the energy levels of the resulting D-A polymers. Thus, with the same donor moiety, the oxadiazole-based polymer was observed to display a slightly lower LUMO energy level than its corresponding thiadiazole-based polymer, attributable to the stronger electro-negativity of oxygen.

**Table 3**  
Electrochemical properties of D-A polymers.

D-A polymer	$E_{\text{ox}}^{\text{onset}}$ (V)	$E_{\text{red}}^{\text{onset}}$ (V)	$^{\text{a}}\text{HOMO}^{\text{ele}}$ (eV)	$^{\text{b}}\text{LUMO}^{\text{opt}}$ (eV)	$\text{LUMO}^{\text{ele}}$ (eV)	$E_{\text{g}}^{\text{ele}}$ (eV)
P1	1.02	−0.77	−5.42	−3.54	−3.63	1.79
P2	0.93	−0.75	−5.33	−3.44	−3.65	1.68
P3	1.00	−0.74	−5.40	−3.51	−3.66	1.74
PF-S	1.42	−0.68	−5.82	−3.67	−3.72	2.10
PF-O	1.34	−0.66	−5.74	−3.61	−3.74	2.00

<sup>a</sup>  $\text{HOMO}^{\text{ele}} = -e(E_{\text{ox}} + 4.4)$  (eV).

<sup>b</sup>  $\text{LUMO}^{\text{opt}} = E_{\text{g}}^{\text{opt}} + E_{\text{HOMO}}$ .

### 3.5. Photovoltaic properties

The photovoltaic properties of the D-A polymers were investigated in bulk heterojunction organic photovoltaic (BHJ-OPV) devices using solar simulator (San\_El Electric, XEC-301S) and Agilent U2722A Modular Source Measure Unit. The device structure had the configuration of ITO/ZnO/active layer/MoO<sub>3</sub>/Ag with the active layer being composed of D-A polymer as the electron donor and PCBM as an electron acceptor. The observed photovoltaic properties, i.e., open circuit voltage ( $V_{\text{oc}}$ ), short circuit current ( $J_{\text{sc}}$ ), fill factor (FF), and power conversion efficiency (PCE) are summarized in Table 4. The PCEs ranging from 0.21% to 2.2% were recorded for these devices. It was noted that the devices with active layer spin cast at spin speed of 1000 rpm displayed higher PCEs than those at spinning speed of 500 rpm (Supporting Information: Fig. S3 and Table S1), which could be attributed to the better film quality of the higher spinning speed. As can be seen from the current density-voltage plots of Fig. 3, the devices using **PF-S** and **PF-O** as donor polymers exhibited much higher  $V_{\text{oc}}$  (0.93 and 0.98 V, respectively) than those with **P1**, **P2**, and **P3** (6.8 V) as donor polymers. These are consistent with their HOMO levels, since  $V_{\text{oc}}$  is proportional to the energy difference between HOMO level of donor and LUMO level of the acceptor (PCBM) [49].

The device with donor polymer, **P2**, afforded the best PCE of 2.2% and  $J_{\text{sc}}$  (4.7 mA/cm<sup>2</sup>) comparable to that of **P1**, which might be due to its higher fill factor (66%). It has been suggested that series resistance ( $R_{\text{s}}$ ) and shunt resistance ( $R_{\text{sh}}$ ) are two of the factors that determine FF [50], thus, a device having lower  $R_{\text{s}}$  and higher  $R_{\text{sh}}$  would yield higher FF and improved PCE. **P2** showed smallest  $R_{\text{s}}$  of 8.2  $\Omega$  cm<sup>2</sup> and a relatively higher  $R_{\text{sh}}$  of 1.9 k $\Omega$  cm<sup>2</sup> than the other four polymers, while **PF-O**, which gave the lowest PCE of 0.21%, had the highest  $R_{\text{s}}$  of 1.9 and  $R_{\text{sh}}$  of 2.3 k $\Omega$  cm<sup>2</sup>. Therefore, the observed PCE values for all five polymers were quite consistent with their FF,  $R_{\text{s}}$  and  $R_{\text{sh}}$  values. The highest PCE for **P2** may be attributed to its lower band-gap and broader absorptions which enable more efficient solar energy harvesting.

The incident photon to current efficiency, IPCE, of the devices for **P1**, **P2** and **P3** (Fig. 4) shows reasonably wide external quantum efficiency (EQE) graphs in the visible region (300–700 nm) with large EQE values in the 300–730 nm region and lower values beyond 730 nm. The **P1** devices exhibited the highest EQE (up to 47.5%) at 380 nm, in good agreement with the result for the highest photocurrent value,  $J_{\text{sc}}$  of 4.71 mA/cm<sup>2</sup> whereas, **P2** and **P3** showed EQE values of 45.5% and 37.4%, respectively.

**Table 4**  
Photovoltaic performance of D-A polymers with PC<sub>70</sub>BM under illumination of AM 1.5G, 940 W/m<sup>2</sup> (Active layer: D-A. Polymer/PC<sub>70</sub>BM (1/2 by weight) with 3% of DIO; 10–12 devices were evaluated for each polymer).

D-A Polymer	$V_{\text{oc}}$ (V)	$J_{\text{sc}}$ (mA/cm <sup>2</sup> )	FF (%)	PCE (%)	$R_{\text{s}}$ (k $\Omega$ cm <sup>2</sup> )	$R_{\text{sh}}$ (k $\Omega$ cm <sup>2</sup> )
P1	0.68	4.7	56	1.9	0.010	1.1
P2	0.68	4.7	66	2.2	$8.2 \times 10^{-3}$	1.9
P3	0.68	3.9	55	1.6	0.019	0.98
PF-S	0.93	1.7	52	0.88	0.80	2.1
PF-O	0.98	0.68	30	0.21	1.9	2.3

### 3.6. Field effect transistor properties

The field-effect transistor properties of D-A polymers were evaluated using a bottom-gate, top-contact transistor configuration. A heavily n-doped silicon wafer <100> with a 300-nm thermally grown silicon dioxide (SiO<sub>2</sub>) was used as the substrate/gate electrode. The surface of SiO<sub>2</sub>/Si substrate was modified with either octyltrichlorosilane (OTS-8) or octadecyltrichlorosilane (OTS-18) to enhance transistor performance. The D-A polymer was dissolved in chlorobenzene (3 mg/mL) and filtered through a syringe fitted with a 10-micron filter. The filtered solution was spin coated on top of OTS-8- or OTS-18-modified SiO<sub>2</sub> surface, vacuum dried at 60 °C for several hours. The devices were optionally annealed at 120 °C for 30 min when required. A series of gold source/drain electrode pairs were deposited by vacuum thermal evaporation through a shadow mask, thus creating a set of OFET devices with various channel length (L) and width (W) dimensions for electrical evaluation. All the polymers had shown p-type semiconductor behavior, and their OFET characteristics are summarized in Tables 5 and 6 for devices treated with OTS-8 and OTS-18, respectively. Typical Transfer and output characteristics as well as hysteresis behavior of OFET devices with **P2** as channel semiconductor on OTS-18-modified substrate are provided in Fig. 5. The transfer and output characteristics and hysteresis behaviors of other D-A polymers are given in Fig. S4/S5 (Supporting Information). The extracted field-effect mobility, current on/off ratio and threshold voltage of OFET devices on OTS-8- and OTS-18-modified substrates are summarized in Tables 5 and 6, respectively. As can be noted, the results showed that **P1**, **P2**, and **P3** gave essentially the same field-effect properties, with **P2** performed slightly better and **P3** slightly poorer. On the other hand, both **PF-S** and **PF-O** gave significantly poorer OFET performance, which may be attributed to the donor moiety, alkylidene-fluorene, being not a strong donor. In addition, we observed that those devices built on ODTS-18-modified SiO<sub>2</sub> substrates afforded much better performance than those on OTS-8-modified substrates. Both mobility and on/ratio are much higher in devices on OTS-18-modified substrates, which are in agreement with the higher efficiency of octadecyl chain in facilitating molecular ordering of the D-A polymers. In addition, noticeable improvements in mobility and on/off ratio were noted after the devices were thermally annealed at 120 °C as thermal treatment was expected to further promote molecular ordering of D-A polymers. The highest mobility of  $2.6 \times 10^{-2}$  cm<sup>2</sup>V<sup>-1</sup>s<sup>-1</sup> and on/ratio of  $3 \times 10^5$  were obtained from devices using **P2** as channel semiconductor.

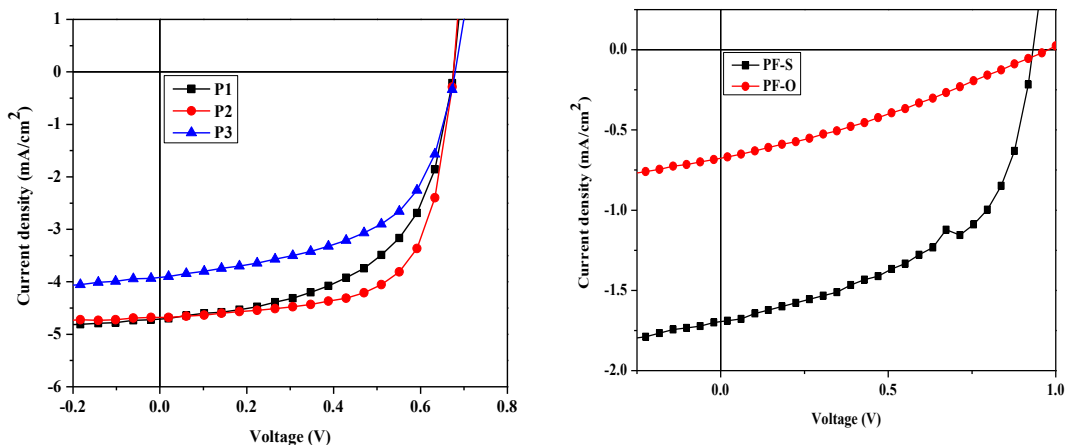


Fig. 3. Current density-voltage of photovoltaic devices with active layer of D-A polymer/PC<sub>70</sub>BM (1/2 by weight) and 3% of DIO additive.

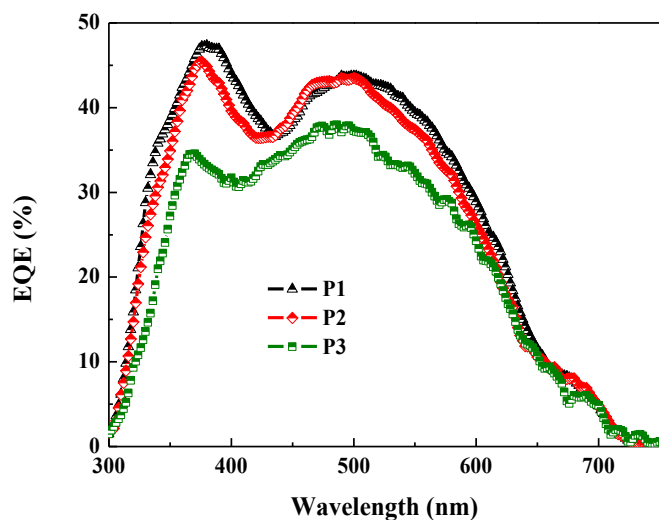


Fig. 4. IPCE spectra of the OPV devices using **P1**, **P2** and **P3** as donor polymers and PC<sub>70</sub>BM as acceptor.

A good correlation between the oxidative potentials of the polymers and the threshold voltages of the corresponding devices was noted. For example, the HOMO levels of **P1**, **P2**, and **P3** are higher than those of **PF-S** and **PF-O**, thus their threshold voltages ( $V_{th}$ ) were more positive ( $-6$  V for **P1**,  $-4$  V for **P2** and  $-10$  V for **P3**) as compared with those of **PF-S** and **PF-O**, which were more negative  $V_{th}$  ( $-14.8$  V for **PF-S** and  $-15$  V for **PF-O**). This was likely related to the hole-injection barrier from the gold contact to the polymer semiconductor as **PF-S** and **PF-O** polymers have deeper HOMO levels ( $-5.82$  to  $-5.74$  eV) which are not energetically compatible with gold which has a work function of  $-5.1$  eV. Interestingly **P1**, **P2**, and **P3** polymers showed very small hysteresis in their transfer characteristics, indicating less trapping in polymer films [51].

The AFM images of pristine films of **P1-3** and **PF-S**, **PF-O** spin-cast on OTS modified Si/SiO<sub>2</sub> substrates from CB solution at 800 rpm and annealed at 120 °C are shown in Fig. S6 (Supporting Information). **P2** formed ordered biocontinuous networks of cylindrical structures, which may contribute to its superior performance among all of the polymers in OFET devices. In contrast to **P2**, both **P1** and **P3** formed relatively smooth films without obvious phase separation. Both **PF-S** and **PF-O** formed noncontinuous spherical aggregates, consistent with their poor performances

Table 5

Performance characteristics of OFET devices with D-A polymer semiconductor on OTS-8-treated substrate fabricated and measured under ambient conditions.

D-A polymer	Average Mobility <sup>a</sup> (cm <sup>2</sup> V <sup>-1</sup> s <sup>-1</sup> )		$V_{th}$ (V)	On/off ratio
	As fabricated, 60 °C	Annealed at 120 °C		
P1	$0.7 \times 10^{-2}$ ( $0.8 \times 10^{-2}$ )	$1.1 \times 10^{-2}$ ( $1.3 \times 10^{-2}$ )	$-6.0$	$2 \times 10^4$
P2	$1.1 \times 10^{-2}$ ( $1.2 \times 10^{-2}$ )	$1.6 \times 10^{-2}$ ( $1.7 \times 10^{-2}$ )	$-4.0$	$6 \times 10^4$
P3	$0.5 \times 10^{-2}$ ( $0.6 \times 10^{-2}$ )	$1.5 \times 10^{-2}$ ( $1.9 \times 10^{-2}$ )	$-10.1$	$3 \times 10^5$
PF-S	$1.6 \times 10^4$	$2.6 \times 10^{-4}$	$-14.8$	$2 \times 10^4$
PF-O	$4 \times 10^4$	$1.1 \times 10^{-3}$	$-15.0$	$5 \times 10^4$

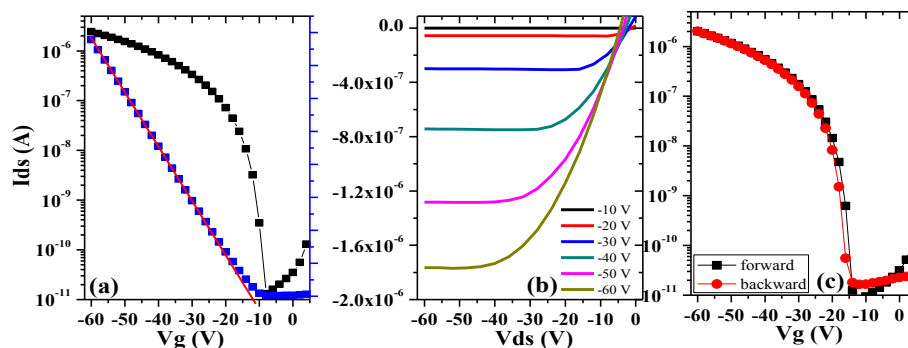
<sup>a</sup> Maximum mobility shown in parentheses.

Table 6

Performance characteristics of OFET devices with D-A polymer semiconductor on OTS-18-treated substrate fabricated and measured under ambient conditions.

D-A polymer	Average Mobility <sup>a</sup> (cm <sup>2</sup> V <sup>-1</sup> s <sup>-1</sup> )		$V_{th}$ (V)	On/off ratio
	As fabricated, 60 °C	Annealed at 120 °C		
P1	$1.5 \times 10^{-2}$ ( $1.7 \times 10^{-2}$ )	$2.3 \times 10^{-2}$ ( $2.4 \times 10^{-2}$ )	$-12.0$	$10^5$
P2	$2.1 \times 10^{-2}$ ( $2.4 \times 10^{-2}$ )	$2.4 \times 10^{-2}$ ( $2.6 \times 10^{-2}$ )	$-12.0$	$3 \times 10^5$
P3	$0.6 \times 10^{-2}$ ( $0.7 \times 10^{-2}$ )	$1.9 \times 10^{-2}$ ( $2.0 \times 10^{-2}$ )	$-7.1$	$3 \times 10^5$

<sup>a</sup> Maximum mobility shown in parentheses.



**Fig. 5.** Typical transfer (a), output characteristics curves (b), and forward/backward gate voltage sweeps (hysteresis) (c) of OFET devices with **P2** as channel semiconductor on OTS-18-modified  $\text{SiO}_2/\text{Si}$  substrate ( $W/L = 1500 \mu\text{m}/160 \mu\text{m}$  devices).

(Table 5) in OFET devices. Their root-mean square (RMS) surface roughness values are **P1** (1.86 nm), **P2** (4.57 nm), **P3** (3.50 nm), **PF-S** (3.93 nm), and **PF-O** (2.52 nm). In addition, one can see that the exchange of S/O atoms did not result in any significant change in film morphology, which is consistent with the results reported by Huang et al. and Shi et al. in similar polymers [30,47].

#### 4. Conclusion

D-A polymers comprising dithienobenzochalcogenodiazole acceptor units alternating with thienothiophene, bithiophene, and alkylidene fluorene donor units were synthesized for evaluation as semiconductor polymers for OPV and OFET devices. The D-A polymers based on thienothiophene and bithiophene structures have exhibited lower optical bandgaps as compared to their alkylidene fluorene analogues. From solution to thin-film state, all polymers exhibited red shifts in their absorption spectra accompanied with the appearance of shoulder peaks, indicating formation of more planar polymer backbone orderings or some *J*-aggregates in their solid states. UV–vis and CV studies revealed that oxadiazole-containing polymers displayed deeper LUMO levels and more red-shifted thin-film absorption spectra when compared to their respective thiadiazole-containing counterparts. Among all the polymers, **P2** provided the highest PCE in OPVs and highest mobility and on/off ratio in OFETs. Also worthy of note is the finding that many of these polymer (i.e., **P1**, **P2** and **P3**) exhibited little hysteresis effects in OFET devices. We believe that the electronic device performance can be further improved through structural and synthesis optimization.

#### Acknowledgments

M.W. is grateful for the start-up funding support of Nanyang Assistant Professorship by Nanyang Technological University. We gratefully acknowledge A\*STAR, Singapore (Grant No. 102 170 0135) and Hong Kong Baptist University Strategic Development fund (SDF13-0531-A02) for financial support. We thank Kai Wang and Marc Courte for help in AFM.

#### Appendix A. Supplementary data

Supplementary data related to this article can be found at <http://dx.doi.org/10.1016/j.dyepig.2016.01.035>.

#### References

- [1] Holliday S, Donaghey JE, McCulloch I. Advances in charge carrier mobilities of semiconducting polymers used in organic transistors. *Chem Mater* 2013;26(1):647–63.
- [2] Guo X, Baumgarten M, Müllen K. Designing  $\pi$ -conjugated polymers for organic electronics. *Prog Polym Sci* 2013;38(12):1832–908.
- [3] Zhao Y, Guo Y, Liu Y. 25th anniversary article: recent advances in n-type and ambipolar organic field-effect transistors. *Adv Mater* 2013;25(38):5372–91.
- [4] Usta H, Facchetti A, Marks TJ. n-Channel semiconductor materials design for organic complementary circuits. *Acc Chem Res* 2011;44(7):501–10.
- [5] Anthony JE, Facchetti A, Heeney M, Marder SR, Zhan X. n-Type organic semiconductors in organic electronics. *Adv Mater* 2010;22(34):3876–92.
- [6] Jung BJ, Tremblay NJ, Yeh M-L, Katz HE. Molecular design and synthetic approaches to electron-transporting organic transistor semiconductors. *Chem Mater* 2010;23(3):568–82.
- [7] Shin RY, Sonar P, Siew PS, Chen Z-K, Sellinger A. Electron-accepting conjugated materials based on 2-vinyl-4, 5-dicyanoimidazoles for application in organic electronics. *J Org Chem* 2009;74(9):3293–8.
- [8] Li J, Zhao Y, Tan HS, Guo Y, Di C-A, Yu G, et al. A stable solution-processed polymer semiconductor with record high-mobility for printed transistors. *Sci Rep* 2012;2.
- [9] Boudreaud P-LT, Najari A, Leclerc M. Processable low-bandgap polymers for photovoltaic applications. *Chem Mater* 2010;23(3):456–69.
- [10] Chen J, Cao Y. Development of novel conjugated donor polymers for high-efficiency bulk-heterojunction photovoltaic devices. *Acc Chem Res* 2009;42(11):1709–18.
- [11] Inganäs O, Zhang F, Andersson MR. Alternating polyfluorenes collect solar light in polymer photovoltaics. *Acc Chem Res* 2009;42(11):1731–9.
- [12] Peet J, Heeger AJ, Bazan GC. “Plastic” solar cells: self-assembly of bulk heterojunction nanomaterials by spontaneous phase separation. *Acc Chem Res* 2009;42(11):1700–8.
- [13] Svensson M, Zhang F, Veenstra SC, Verhees WJ, Hummelen JC, Kroon JM, et al. High-performance polymer solar cells of an alternating polyfluorene copolymer and a fullerene derivative. *Adv Mater* 2003;15(12):988–91.
- [14] Blouin N, Michaud A, Leclerc M. A low-bandgap poly(2, 7-carbazole) derivative for use in high-performance solar cells. *Adv Mater* 2007;19(17):2295–300.
- [15] Peet J, Kim J, Coates NE, Ma WL, Moses D, Heeger AJ, et al. Efficiency enhancement in low-bandgap polymer solar cells by processing with alkane dithiols. *Nat Mater* 2007;6(7):497–500.
- [16] Wang E, Wang L, Lan L, Luo C, Zhuang W, Peng J, et al. High-performance polymer heterojunction solar cells of a polysilfluorene derivative. *Appl Phys Lett* 2008;92(3):033307–13.
- [17] Nie W, MacNeill CM, Li Y, Noftle RE, Carroll DL, Coffin R. A soluble high molecular weight copolymer of benzo [1, 2-b: 4, 5-b'] dithiophene and benzoxadiazole for efficient organic photovoltaics. *Macromol Rapid Commun* 2011;32(15):1163–8.
- [18] Zhang L, He C, Chen J, Yuan P, Huang L, Zhang C, et al. Bulk-heterojunction solar cells with benzotriazole-based copolymers as electron donors: largely improved photovoltaic parameters by using PFN/Al bilayer cathode. *Macromolecules* 2010;43(23):9771–8.
- [19] Zhao W, Cai W, Xu R, Yang W, Gong X, Wu H, et al. Novel conjugated alternating copolymer based on 2, 7-carbazole and 2, 1, 3-benzoselenadiazole. *Polymer* 2010;51(14):3196–202.
- [20] Blouin N, Michaud A, Gendron D, Wakim S, Blair E, Neagu-Plesu R, et al. Toward a rational design of poly(2, 7-carbazole) derivatives for solar cells. *J Am Chem Soc* 2008;130(2):732–42.
- [21] Gendron D, Morin PO, Najari A, Leclerc M. Synthesis of new pyridazine-based monomers and related polymers for photovoltaic applications. *Macromol Rapid Commun* 2010;31(12):1090–4.
- [22] Liu Y, Zhao J, Li Z, Mu C, Ma W, Hu H, et al. Aggregation and morphology control enables multiple cases of high-efficiency polymer solar cells. *Nat Commun* 2014;5.
- [23] Xiao K, Liu Y, Qi T, Zhang W, Wang F, Gao J, et al. A highly  $\pi$ -stacked organic semiconductor for field-effect transistors based on linearly condensed pentathienoacene. *J Am Chem Soc* 2005;127(38):13281–6.

- [24] Zhang S, Guo Y, Zhang Y, Liu R, Li Q, Zhan X, et al. Synthesis, self-assembly, and solution-processed nanoribbon field-effect transistor of a fused-nine-ring thienoacene. *Chem Commun* 2010;46(16):2841–3.
- [25] Wu W, Liu Y, Zhu D.  $\pi$ -Conjugated molecules with fused rings for organic field-effect transistors: design, synthesis and applications. *Chem Soc Rev* 2010;39(5):1489–502.
- [26] Liu Y, Liu Y, Zhan X. High-mobility conjugated polymers based on fused-thiophene building blocks. *Macromol Chem Phys* 2011;212(5):428–43.
- [27] Wang H, Shi Q, Lin Y, Fan H, Cheng P, Zhan X, et al. Conjugated polymers based on a new building block: dithienophthalimide. *Macromolecules* 2011;44(11):4213–21.
- [28] Mei C-Y, Liang L, Zhao F-G, Wang J-T, Yu L-F, Li Y-X, et al. A family of Donor–Acceptor photovoltaic polymers with fused 4, 7-Dithienyl-2, 1, 3-benzothiadiazole units: effect of structural fusion and side chains. *Macromolecules* 2013;46(19):7920–31.
- [29] Hu S, Bao X, Liu Z, Wang T, Du Z, Wen S, et al. Benzothiadiazole [1, 2-b: 4, 3-b'] dithiophene, a new ladder-type multifused block: synthesis and photovoltaic application. *Org Electron* 2014;15(12):3601–8.
- [30] Huang J, Zhu Y, Chen J, Zhang L, Peng J, Cao Y. Dithienobenzothiadiazole-based conjugated polymer: processing solvent-relied interchain aggregation and device performances in field-effect transistors and polymer solar cells. *Macromol Rapid Commun* 2014;35(22):1960–7.
- [31] Park HJ, Lee Y, Jo JW, Jo WH. Synthesis of a low bandgap polymer based on a thiadiazolo-indolo [3, 2-b] carbazole derivative for enhancement of open circuit voltage of polymer solar cells. *Polym Chem* 2012;3(10):2928–32.
- [32] Cheng Y-J, Ho Y-J, Chen C-H, Kao W-S, Wu C-E, Hsu S-L, et al. Synthesis, photophysical and photovoltaic properties of conjugated polymers containing fused Donor–Acceptor dithienopyrrolobenzothiadiazole and dithienopyrroloquinoline arenes. *Macromolecules* 2012;45(6):2690–8.
- [33] Planells M, Nikolka M, Hurhangee M, Tuladhar PS, White AJ, Durrant JR, et al. The effect of thiadiazole out-backbone displacement in indacenodithiophene semiconductor polymers. *J Mater Chem C* 2014;2(41):8789–95.
- [34] Efrem A, Lim C-J, Lu Y, Ng S-C. Synthesis and characterization of dithienobenzothiadiazole-based donor–acceptor conjugated polymers for organic solar cell applications. *Tetrahedron Lett* 2014;55(35):4849–52.
- [35] Jiang J-M, Yang P-A, Hsieh T-H, Wei K-H. Crystalline low-band gap polymers comprising thiophene and 2, 1, 3-benzooxadiazole units for bulk heterojunction solar cells. *Macromolecules* 2011;44(23):9155–63.
- [36] Liu B, Chen X, Zou Y, Xiao L, Xu X, He Y, et al. Benzo [1, 2-b: 4, 5-b'] difuran-based donor–acceptor copolymers for polymer solar cells. *Macromolecules* 2012;45(17):6898–905.
- [37] Jiang JM, Yang PA, Yu CM, Lin HK, Huang KC, Wei KH. The new low-band gap polymers comprising C-, Si-, or N-bridged dithiophene and alkoxy-modified 2, 1, 3-benzooxadiazole units for bulk heterojunction solar cells. *Journal of Polymer Science Part A. Polym Chem* 2012;50(19):3960–9.
- [38] Bijleveld JC, Shahid M, Gilot J, Wienk MM, Janssen RA. Copolymers of cyclopentadithiophene and electron-deficient aromatic units designed for photovoltaic applications. *Adv Funct Mater* 2009;19(20):3262–70.
- [39] Padhy H, Huang JH, Sahu D, Patra D, Kekuda D, Chu CW, et al. Synthesis and applications of low-bandgap conjugated polymers containing phenothiazine donor and various benzodiazole acceptors for polymer solar cells. *J Polym Sci Part A Polym Chem* 2010;48(21):4823–34.
- [40] Jiang J-M, Yang P-A, Chen H-C, Wei K-H. Synthesis, characterization, and photovoltaic properties of a low-bandgap copolymer based on 2, 1, 3-benzooxadiazole. *Chem Commun* 2011;47(31):8877–9.
- [41] Lan S-C, Yang P-A, Zhu M-J, Yu C-M, Jiang J-M, Wei K-H. Thiophene spacers impart crystallinity and enhance the efficiency of benzotrithiophene-based conjugated polymers for bulk heterojunction photovoltaics. *Polym Chem* 2013;4(4):1132–40.
- [42] Wang X, Jiang P, Chen Y, Luo H, Zhang Z, Wang H, et al. Thieno [3, 2-b] thiophene-bridged D– $\pi$ -A polymer semiconductor based on benzo [1, 2-b: 4, 5-b'] dithiophene and benzoxadiazole. *Macromolecules* 2013;46(12):4805–12.
- [43] Ni J-S, You J-H, Hung W-I, Kao W-S, Chou H-H, Lin JT. Organic dyes incorporating the dithieno [3', 2': 3, 4; 2'', 3'': 5, 6] benzo [1, 2-c] furazan moiety for dye-sensitized solar cells. *ACS Appl Mater Interfaces* 2014;6(24):22612–21.
- [44] Casalini R, Tsang SW, Deininger JJ, Arroyave FA, Reynolds JR, So F. Investigation of the role of the acceptor molecule in bulk heterojunction photovoltaic cells using impedance spectroscopy. *J Phys Chem C* 2013;117(27):13798–804.
- [45] Choi M-H, Song KW, Moon DK. Alkylidene-fluorene–isoidigo copolymers with an optimized molecular conformation for spacer manipulation,  $\pi$ – $\pi$  stacking and their application in efficient photovoltaic devices. *Polym Chem* 2015;6(14):2636–46.
- [46] Arroyave FA, Richard CA, Reynolds JR. Efficient synthesis of benzo [1, 2-b: 6, 5-b'] dithiophene-4, 5-dione (BDTD) and its chemical transformations into precursors for  $\pi$ -conjugated materials. *Org Lett* 2012;14(24):6138–41.
- [47] Shi S, Shi K, Chen S, Qu R, Wang L, Wang M, et al. Synthesis, characterization, and organic field-effect transistors study of conjugated D–A copolymers based on dialkylated naphtho [1, 2-b: 5, 6-b'] dithiophene/naphtho [1, 2-b: 5, 6-b'] difuran and benzodithiadiazole/benzoxadiazole. *J Polym Sci Part A Polym Chem* 2014;52(17):2465–76.
- [48] Lei T, Cao Y, Zhou X, Peng Y, Bian J, Pei J. Systematic investigation of isoidigo-based polymeric field-effect transistors: design strategy and impact of polymer symmetry and backbone curvature. *Chem Mater* 2012;24(10):1762–70.
- [49] Scharber MC, Mühlbacher D, Koppe M, Denk P, Waldauf C, Heeger AJ, et al. Design rules for donors in bulk-heterojunction solar cells—Towards 10% energy-conversion efficiency. *Adv Mater* 2006;18(6):789–94.
- [50] Qi B, Wang J. Fill factor in organic solar cells. *Phys Chem Chem Phys* 2013;15(23):8972–82.
- [51] Osaka I, Zhang R, Sauvé G, Smilgies D-M, Kowalewski T, McCullough RD. High-lamellar ordering and amorphous-like  $\pi$ -network in short-chain thiazolothiazole–thiophene copolymers Lead to high mobilities. *J Am Chem Soc* 2009;131(7):2521–9.